Development 129, 5753-5765

doi:10.1242/dev.00178

Mouse dispatched mutants fail to distribute hedgehog proteins and are defective in hedgehog signaling

Takatoshi Kawakami*, T'Nay Kawcak*, Ya-Jun Li, Wanhui Zhang, Yongmei Hu and Pao-Tien Chuang†

Cardiovascular Research Institute, University of California, San Francisco, CA 94143, USA

*These authors contributed equally to this work
†Author for correspondence (e-mail: chuang@cvrimail.ucsf.edu)

Accepted 30 September 2002

SUMMARY

Hedgehog (Hh) signaling plays a major role in multiple aspects of embryonic development, which involves both short- and long-range signaling from localized Hh sources. One unusual aspect of Hh signaling is the autoproteolytic processing of Hh followed by lipid modification. As a consequence, the N-terminal fragment of Hh becomes membrane anchored on the cell surface of Hh-producing cells. A key issue in Hh signaling is to understand the molecular mechanisms by which lipid-modified Hh protein is transported from its sites of synthesis and subsequently moves through the morphogenetic field. The dispatched gene, which encodes a putative multipass membrane protein, was initially identified in *Drosophila* and is required in Hh-producing cells, where it facilitates the transport of cholesterol-modified Hh. We report the identification of the mouse dispatched (*Disp*) gene and a phenotypic analysis of *Disp* mutant mice. *Disp*-null mice phenocopy mice deficient in the smoothened gene, an essential component for Hh reception, suggesting that *Disp* is essential for Hh signaling. This conclusion was further supported by a detailed molecular analysis of *Disp* knockout mice, which exhibit defects characteristic of loss of Hh signaling. We also provide evidence that *Disp* is not required for Hh protein synthesis or processing, but rather for the movement of Hh protein from its sites of synthesis in mice. Taken together, our results reveal a conserved mechanism of Hh protein movement in Hh-producing cells that is essential for proper Hh signaling.

Key words: Dispatched, Hedgehog, Mouse, Protein transport

INTRODUCTION

Hedgehog (Hh) signaling plays a key role in inductive interactions in many tissues during vertebrate development (reviewed by Chuang and Kornberg, 2000; Ingham and McMahon, 2001). This process involves both short- and long-range signaling from a localized Hh source. Molecular studies of the Hh pathway have shown that Hh signaling is capable of exerting long-range signaling activity over a distance of tens of cell diameters and inducing distinct cell fates in a dose-dependent manner. For example, sonic hedgehog (*Shh*) expression in the notochord and floor plate patterns the ventral neural tube as well as the sclerotome of the somites (Chiang et al., 1996; Echelard et al., 1993; Fan and Tessier-Lavigne, 1994; Marti et al., 1995a; Roelink et al., 1995). Similarly, *Shh* expression in the zone of polarizing activity (ZPA) specifies digit identity along the anteroposterior axis of the developing limbs (Chiang et al., 1996; Lewis et al., 2001; Riddle et al., 1993; Yang et al., 1997).

Extensively studies on Hh signaling in both invertebrates and vertebrates have led to a prevailing model of Hh reception. Hh signal is transduced through hedgehog binding to patched 1 (Ptch), a multipass transmembrane protein (reviewed by Ingham and McMahon, 2001; Kalderon, 2000). Genetic and molecular studies suggest that Ptch inhibits the signaling activity of smoothened (Smo), a seven transmembrane protein that shares sequence similarity with G-protein-coupled receptors (reviewed by Ingham and McMahon, 2001; Kalderon, 2000). Though the molecular mechanism remains to be elucidated, Hh binding to Ptch appears to relieve the Ptch-mediated repression of Smo. As a consequence, activated Smo can initiate the signaling cascade, turning on transcription of key Hh targets.

An attractive model to account for the activity of Hh is the generation of a Hh protein concentration gradient, which provides positional information in the morphogenetic field. The mechanism by which Hh protein moves across tens of cell diameters is not obvious because of the fact that Hh protein is membrane anchored through lipid modification. The Hh protein precursor undergoes autoproteolysis to generate an N-terminal signaling fragment (Shh-N) (Bumcrot et al., 1995; Lee et al., 1994), followed by two types of post-translational modification. A cholesterol molecule is covalently attached to the C terminus of Shh-N (Porter et al., 1996a; Porter et al., 1996b) and a palmitoyl group is added to the N-terminus of Shh-N (Pepinsky et al., 1998) (the resulting lipid-modified form of Shh-N will be denoted as Shh-Np). The role of lipid modification in Hh signaling is not completely understood, but in vitro studies have shown that Shh-Np becomes membrane anchored as a consequence of lipid modification. It is

conceivable that an important step in Hh signaling is to release the membrane-anchored Hh from the Hh-producing cells to allow for subsequent 'movement' through the morphogenetic field. Interestingly, movement of lipid-modified Hh in *Drosophila* depends on the activity of *tout velou* (*ttv*) in Hh-receiving cells (Bellaiche et al., 1998). *ttv* encodes a glycosaminoglycan transferase, suggesting TTV generates a proteoglycan that may mediate the transfer of Hh protein between cells. The role of *ttv* vertebrate homologs, the Ext genes (Stickens et al., 1996), in Hh signaling has not yet been established.

Some insight into the process of Hh release from Hh-producing cells came from the identification of the *dispatched* (*disp*) gene in *Drosophila* that is predicted to encode a twelve-pass transmembrane protein and is required in Hh-producing cells to transport lipid-modified Hh protein (Burke et al., 1999). *Drosophila* mutants in the *disp* gene display phenotypes reminiscent of *hh* mutants as Hh protein, instead of moving out of Hh-producing cells, accumulates to a higher level in these cells (Burke et al., 1999). Disp exhibits sequence similarity to an emerging family of multipass membrane proteins, including Ptch, all of which contain a characteristic sterol-sensing domain (SSD) (reviewed by Kuwabara and Labouesse, 2002). These observations suggest that Hh movement is closely linked to lipid modification and likely employs novel cellular mechanisms in releasing and transporting a membrane-anchored cell surface protein. However, the biochemical mechanisms by which Disp facilitates Hh movement remain unknown. To address the issue of Hh movement in vertebrates, we report the identification of the mammalian dispatched gene and studies aimed to understand its role in Hh protein transport during vertebrate embryonic development.

MATERIALS AND METHODS

Standard molecular biology techniques were performed as described (Sambrook and Russell, 2001).

Cloning of mouse dispatched (*Disp*) cDNA

A mouse EST clone (IMAGE 1430982) containing sequence similarity to the *Drosophila disp* gene was used to screen a mouse embryonic cDNA library and several partial *Disp* cDNAs were obtained. The 5′ end of the *Disp* cDNA was obtained by RT-PCR. A full-length *Disp* cDNA (4721 bp) was acquired by ligating together restriction fragments of partial cDNAs. The GenBank Accession Number for mouse *Disp* cDNA is AY150577.

Generation of *Disp* null mice

Mouse *Disp* cDNA was used to screen a mouse 129/SvJ genomic library. To construct a positive/negative targeting vector for removing exon 8 of the *Disp* gene (the resulting allele is designated *DispΔ E8*), a 2.7 kb fragment containing sequences upstream of intron 7 was used as the 5′ region of homology (Fig. 3A). A 3.5 kb fragment containing sequences downstream of exon 8 was used as the 3′ region of homology and was inserted upstream of the MC1-*tk*-pA cassette (see Fig. 3A). A PGK-*neo*-pA cassette was inserted between the 5′ and 3′ homology regions and replaces the seventh intron and eighth exon of the *Disp* gene (Fig. 3A). E14Tg2A.4 (E14) feeder-independent ES cells (Nichols et al., 1990) were electroporated with a *Sal*I-linearized targeting vector and selected in G418 and FIAU as described (Joyner, 2000). Heterozygous E14 ES cells were injected into blastocysts of C57BL/6 strain mice to generate germline chimeras. Chimeric males were mated with C57BL/6, 129/Sv, 129/Ola or Swiss-Webster females (to maintain the *Disp* mutant allele in different genetic backgrounds) and heterozygous animals were identified by Southern blotting of tail-tip DNA (Fig. 3B).

Histology and in situ hybridization

Histological analysis, whole-mount in situ hybridization using digoxigenin-labeled probes and section in situ hybridization using ^{33}P-labeled riboprobes were performed as described (Wilkinson and Nieto, 1993). The mouse *Disp* in situ probe encompasses the last kb of the *Disp* cDNA.

Western blotting

We collected wild-type, *DispΔ E8*$^{+/-}$ and *DispΔ E8*$^{-/-}$ embryos at 9.5 dpc (genotypes confirmed by Southern blotting) for western blotting to detect the processing event of Shh. In addition, we transfected COS7 cells, using Lipofectamine Plus reagent (Invitrogen), with expression constructs, which encode either the full-length Shh or the N-terminal fragment of Shh (Shh-N) without post-translational modifications. Transfected cells were harvested 2 days after transfection. To control for the specificity of Shh antibodies, we also collected *Shh* mutant embryos at a stage similar to that of *DispΔ E8*$^{-/-}$ embryos. COS7 cells or 9.5 dpc mouse embryos were lysed in buffer containing 50 mM Tris (pH 8.0), 150 mM NaCl, 2 mM EDTA, 1% Triton X-100 (v/v), 0.5 mM DTT, 1 mM PMSF and 2 μg/ml each of aprotinin, leupeptin and pepstatin A. Insoluble materials were sedimented by centrifugation at 20,000 ***g*** for 30 minutes at 4°C. The supernatants were transferred into a fresh tube and the samples were separated on 15% SDS-PAGE and transferred onto PVDF membranes for immunoblotting (Harlow and Lane, 1999). The membranes were blocked in 10% w/v fat-free milk powder in phosphate buffered saline (PBS) containing 0.1% Tween 20 overnight and incubated with primary antibody against Shh for 2 hours. The membranes were incubated with secondary antibodies followed by chemiluminescent detection according to manufacturer's instructions (ECL, Amersham Pharmacia Biotech).

Immunohistochemistry

We followed a protocol kindly provided by Dr Gritli-Linde (Gritli-Linde et al., 2001) with some minor modifications. The embryos were fixed overnight in Sainte Marie's fixative (95% ethanol, 1% acetic acid) at 4°C. After washing the embryos three times, 30 minutes each, in 95% ethanol, we proceeded to paraffin embedding and sectioning at 5 μM. Tissues were dewaxed in xylene twice, 5 minutes each and rehydrated to water by taking through 100% ethanol twice, 5 minutes each, 95% ethanol twice, 5 minutes each and PBS once for 5 minutes. The endogenous peroxidases were blocked by incubating the slides in 3% H_2O_2 in methanol for 10 minutes in the dark at room temperature. The slides were rinsed in PBS three times, 5 minutes each, and the nonspecific staining was blocked by incubating the slides in PBS with 5% sheep serum, 0.2% BSA and 0.1% Triton X-100 for 40 minutes at room temperature. Slides were incubated overnight at 4°C with the primary antibody (anti-Shh) diluted 1:500 in PBS with 0.2% BSA and 0.1% Triton X-100 in a humidified chamber. The signal was amplified using a Tyramide signal amplification kit (TSA Biotin kit NEL700 or 700A from PerkinElmer). We followed a modified version of the manufacturer's protocol outlined below. The slides were rinsed three times, 5 minutes each, in TNT (0.1M Tris, pH 7.5, 0.15 M NaCl, 0.025% Tween 20). Slides were then incubated with goat anti-rabbit biotinylated secondary antibody at 5 μg/ml (Vector laboratories) in TNT solution containing 2% w/v fat-free milk powder for 45 minutes at room temperature in a humidified chamber. Slides were rinsed three times, 5 minutes each, in TNT solution. The slides were incubated for 30 minutes in TNB buffer (0.1 M Tris, pH 7.5, 0.15 M NaCl, 0.5% blocking reagent) in the dark at room temperature in a humidified chamber. The slides were incubated for 30 minutes with SA-HRP diluted 1:100 in TNB buffer at room temperature in the dark in a

humidified chamber. The slides were rinsed three times, 5 minutes each, in TNT solution and they were incubated in the Biotinyl-tyramide amplification reagent diluted to a working concentration of 1:50 for exactly 9 minutes in the dark. The slides were rinsed three times, 5 minutes each, in TNT solution and incubated with SA-HRP diluted 1:100 in TNB buffer for 30 minutes at room temperature in the dark and in a humidified chamber. Next, The slides were rinsed three times, 5 minutes each and once for 2 minutes, in TNT solution and developed in DAB solution (Vector laboratories) for 3-20 minutes. Finally, the slides were rinsed in PBS for 5 minutes and counterstained using 0.5% Toluidine Blue with 10 mM sodium acetate (pH 4.6).

RESULTS

Cloning of the mouse dispatched (*Disp*) gene

We performed sequence analysis of the mouse genome and identified two genes with significant sequence similarity to the *Drosophila disp* gene (Fig. 1). One of these genes shares greater sequence similarity with *disp* and is likely the mouse ortholog of *disp* (which will be referred to as *Disp* throughout this report), while the other (referred to as *Disp-related*) is probably a more distant member of the family. We isolated full-length *Disp* cDNA clones by screening a mouse embryonic cDNA library using a *Disp* EST clone (IMAGE 1430982) as a probe in hybridization, as well as amplifying fragments of *Disp* cDNAs by polymerase chain reaction (PCR). The complete *Disp* cDNA (4721bp) encodes a predicted protein of 1521 amino acids with a relative molecular mass of 170,047 (Fig. 1A). Both *Disp* and *Disp-related* encode proteins with twelve predicted membrane-spanning domains as well as stretches of sequences similar to a conserved domain known as the sterol-sensing domain (SSD) (Fig. 1A). Proteins containing the SSD include several classes of proteins that are involved in different aspects of cholesterol homeostasis or cholesterol-linked signaling (Fig. 1B) (reviewed by Kuwabara and Labouesse, 2002). Notably, Ptch, the Hh receptor, also contains an SSD. The function of the SSD is not well understood but it has been suggested that SSD plays a role in vesicular trafficking/cargo transport in relation to sterol and/or lipoprotein concentration.

The expression domains of *Disp* during mouse embryogenesis overlap with those of *Shh* and *Ihh*

As a first step towards understanding the potential role that *Disp* plays in Hh signaling, we examined the temporal and spatial expression patterns of *Disp* in mouse embryos collected from 7.5 days post coitum (dpc) to 18.5 dpc. *Shh* is first detected at late streak stages of gastrulation (~7.75 dpc) in the midline mesoderm arising from the node (Echelard et al., 1993) (Fig. 2A). Weak *Ihh* expression is also detected in the posterior part of the node at 7.75-8.0 dpc (Zhang et al., 2001). Genetic analysis demonstrated that *Shh* and *Ihh* play partially redundant roles in Hh signaling in the mouse node (Zhang et al., 2001). At 7.75 dpc, *Disp* is barely detectable by whole-mount in situ hybridization (Fig. 2B) but a ~4.7 kb *Disp* transcript could be detected at this stage on a Northern blot (data not shown). By late-headfold stage just prior to somite formation, *Shh* expression is detected in the node and head process (Echelard et al., 1993) (Fig. 2C). At this stage, *Disp* is only very weakly expressed in cells immediately adjacent to the midline mesoderm (arrowheads in Fig. 2D) as well as at junctions between neural and surface ectoderm (arrows in Fig. 2D). Subsequently, *Shh* expression is detected in several signaling centers, including the notochord, floor plate and ZPA of the limb and in several endoderm derivatives (Echelard et al., 1993). As somites form (~8 dpc) and the embryonic axis extends caudally, the notochord, which represents the caudal extension of the head process, also expresses *Shh*. *Disp* is initially weakly activated in the notochord and its expression is upregulated by 9.5 dpc (Fig. 2I,M). By 8.5 dpc, when *Shh* is induced in the floor plate at the ventral midline, *Disp* expression is only very faintly expressed in the floor plate at this stage as well as at later stages (Fig. 2I,M and data not shown). At ~9.5 dpc *Shh* is activated in the ZPA of the forelimb (Echelard et al., 1993) and *Disp* is broadly expressed throughout the limb mesenchyme as well in the apical ectodermal ridge (AER) (Fig. 2H-J). Expression levels of *Shh* in the ZPA increase from 9.5 to 10.5 dpc (Echelard et al., 1993). At 10.5 dpc, *Disp* expression in both fore- and hindlimb is still broad, but its expression is downregulated both in ZPA and surrounding regions (arrow in Fig. 2L). Expression of *Disp* is also detected in the somite and branchial arches (Fig. 2H,M,L).

At later stages of development, *Ihh* expression is detected in developing chondrocytes. *Ihh* expression is first detected at 12.5 dpc in chondrocytes in the center of cartilage condensation of long bones (Bitgood and McMahon, 1995; St-Jacques et al., 1999). At 13.5 dpc, *Ihh* expression is downregulated in the more mature central cells that are undergoing hypertrophy (Bitgood and McMahon, 1995; St-Jacques et al., 1999). At this stage, the expression domain of *Disp* largely overlaps with that of *Ihh* (data not shown). In addition, a strong *Disp* expression domain was detected in the articular chondrocytes facing the joint cavity (data not shown). At later stages, *Ihh* expression is restricted to the prehypertrophic chondrocytes between the zones of proliferating and hypertrophic chondrocytes (Bitgood and McMahon, 1995; St-Jacques et al., 1999) (Fig. 2O); *Disp* expression remains associated with *Ihh* expression in the prehypertrophic condrocytes in addition to maintaining its strong expression in the articular chondrocytes (Fig. 2P). Taken together, these findings suggest a potential role of *Disp* in Hh signaling since its expression domains overlap with those of both *Shh* and *Ihh* during early mouse embryogenesis.

Mouse embryos deficient in the *Disp* gene do not survive beyond 9.5 dpc and resemble *Smo* mutant embryos

To better understand the role *Disp* plays in Hh signaling, we generated a null allele of *Disp* using gene targeting in mice. The *Disp* gene is located on mouse chromosome 1 and the genomic locus consists of eight exons. The eighth exon encodes the last 1193 amino acids of Disp protein, which include all twelve predicted transmembrane domains (Fig. 3A). We targeted the eighth exon to generate a null allele of the *Disp* gene (designated *DispΔ E8*) (Fig. 3B). The gross morphology of homozygous *DispΔ E8* mutant embryos at 9.5 dpc (Fig. 4B) is remarkably similar to embryos deficient in the *Smo* gene (Zhang et al., 2001) (Fig. 4C). Furthermore, similar to *Smo* mutants, homozygous *DispΔ E8* mutants do not survive beyond 9.5 dpc. By contrast, *DispΔ E8* heterozygous embryos cannot be distinguished from their wild-type littermates (data not shown). *DispΔ E8* mutants exhibit cyclopia and holoprosencephaly. In

A

```
MAVISGSDSVLLSNGSISTSTSNPSPLSPSDGDLPAQHLGPRETPRTKASPNGCLQLNGTVKSSFLPLDNQRTPQTPTQCCHPCP   86
YHHPVSSHSNHQECHPEAGLAASPALASCRMQPHSEYSASLCPNHSPVYQAAHCLQPSPSFCLHHPWPDHFQHQPVRQHLTIIRP   171
SRPFKFPRSYAALLADWPVVVLGMCTLLIVVCALVGVLVPELPDFSDPLLGFEPRGTTIGQRLVTWNNMMRNTGYKATLANYPYK   256
YAEEQARSHRDDRWSDDHHERERREVDWNFQKDSFFCDVPSDGYSRVVFASAGGETLWNLPAIKSMCDVDNSRIRSHPQFSDLCQ   341
RTTAVSCCPSWTLGNYIAILNNRSSCQKIVERDVSHTLKLLRTCAKHYQNGTLGPDCWDKAARRKDQLKCTNVPRKCTKYNAVYQ   426
ILHYLVDKDFMTPKTADYAVPALKYSMLFSPTEKGESMMNIYLDNFENWNSSDGITTVTGIEFGIKHSLFQDYLLMDTVYPAIAI   511
AIVLLIMCVYTKSMFITLMTMFAIISSLIVSYFLYRVVFNFEFFPFMNLTALIILVGIGADDAFVLCDVWNYTKFDKPRAETSEA   596
VSVTLQHAALSMFVTSFTTAAAFYANYVSNITAIRCFGVYAGTAILVNYVLMVTWLPAVIVLHERYLLNIFTCFRKPQPQAYDKS   681
CWAVLCQKCRRVLFAVSEASRIFFEKVLPCIVIKFRYLWLIWFLALTVGGAYIVCVNPKMKLPSLELSEFQVFRSSHPFERYDAE   766
FKKLFMFERVHHGEELHMPITVIWGVSPEDSGDPLNPKSKGELTLDSTFNIASPASQAWILHFCQKLRNQTFFHQTEQQDFTSCF   851
IETFKQWMENQDCDEPALYPCCSHCSFPYKQEVFELCIKKAIMELDRSTGYHLNNKTPGPRFDINDTIRAVVLEFQSTFLFTLAY   936
EKMQQFYKEVDSWISHELSSAPEGLSRGWFVSNLEFYDLQDSLSDGTLIAMGLSVAVAFSVMLLTTWNIIISLYAIVSIAGTIFV   1020
TVGSLVLLGWELNVLESVTISVAVGLSVDFAVHYGVAYRLAPDPDREGKVIFSLSRMGSAIAMAALTTFVAGAMMMPSTVLAYT   1104
QLGTFMMLVMCVSWAFATFFFQCLCRCLGPQGTCGQIPFPTKLQCSPFSHTLSARPGDRGPSKTHAASAYSVDARGQKSQLEHEF   1190
YELQPLASHSCTSSEKTTYEEPHTCSEFFNGQAKNLRMPVPAAYSSELTKSPSSEPGSALLQSCLEQDTVCHFSLNPRCNCRDAY   1275
THLQYGLPEIHCQQMGDSLCHKCASTAGGFVQIQNSVAPLKASHQAAEGLLHPAQHMLPPGMQNSRPRNFFLHSVQHFQAQENLG   1360
RTSTHSTDERLPRTAELSPPPSDSRSTESFQRACCHPENNQRRLCKSRDPGDTEGSGGTKSKVSGLPNQTDEEEKQVEPSLLQTD   1445
ETVNSEHLNHNESNFTFSHLPGEAGCRSCPNSPQSCRSIMRSKCGTEDCQTPNLEANVPAVPTHSDLSGESLLIKTL           1521
Transmembrane Domain  SSD Domain
```

B

```
Consensus sequence          --------Y-SMFLYLMLALGVID--------S--SLGLAGFLYVA-S-AFSLGLFPLVGLTAT------

Disp Mouse SSD 523-657     ----------SMFITLMTMFAIIS----------SLIVSYFLYRV---VFNFEFFPFMNLTAL------ 40
Disp Human SSD 507-643      --------LRSLFLTLMVLLGVLG----------SLLVAFFLYQV---AFRMAYFPFVNLAAL------ 42
Disp Dros SSD 468-624       ----------SAFITLMSCVAICF----------SLGLAYFFYAI---VLEFEFFPYMNLLAV------ 40
CHE14 SSD 351-472           ----------AFVVILLLALSVVG----------ALGVYSLF------T---DEFPLLNLVTF------ 34
KIAA 1742 Mouse SSD 407-543 --------LRSLFLTLMVLLGVLG----------SLLVAFFLYQV---AFRMAYFPFVNLAAL------ 42
PTC1 Mouse  SSD 424-584     SVIRVASGYLLMLAYACLTMLRWDCS-----KSQGAVGLAGVLLVALSVAAGLGLCSLIGISFN-AATTQ 64
PTC1 Human  SSD 438-598     SVIRVASGYLLMLAYACLTMLRWDCS-----KSQGAVGLAGVLLVALSVAAGLGLCSLIGISFN-AATTQ 64
PTC2 Mouse SSD 991-1113     ------------LIVLVLAMMTVE----------LFGIMGFLG------IKLSAIPVVILVAS------ 35
PTC2 Human SSD 394-552      SAARVVGGYLLMLAYACVTMLRWDCA-----QSQGSVGLAGVLLVALAVASGLGLCALLGITFN-AATTQ 64
SCAP Human SSD 284-442      ELIPLVTTYIILFAYIYFSTRKID-----MVKSKWGLALAAVVTVLSSLLMSVGLCTLFGLTPT-LNGGE 64
NPC1 Mouse SSD 621-786      DVFTVIISYVVMFLYISLALGHIQSCSRLLVDSKISLGIAGILIVLSSVACSLGIFSYMGMPLT-LIVIE 69
NPC1 Human SSD 620-785      DVFTVVISYAIMFLYISLALGHIKSCRRLLVDSKVSLGIAGILIVLSSVACSLGVFSYIGLPLT-LIVIE 69
HMGCR Human SSD 61-218      DIIILTITRCIAILYIYFQFQNLR-----QLGSKYILGIAGLFTIFSSFVFSTVVIHFLDKELTGLN--E 63

Consensus sequence          --PFLLLGIGVDDVFLLADAFL------LSN------------SQLEVR-------QRVGRTLGHTGASM

Disp Mouse SSD 523-657     ---IILVGIGADDAFVLCDVWN---YTKFDK------------PRAETS-------EAVSVTLQHAALSM 85
Disp Human SSD 507-643      ---LLLSSVCANHTLIFFDLWR------LSK------------SQLPSG----GLAQRVGRTMHHFGYLL 87
Disp Dros SSD 468-624       ---VVIIGIGADDVFLFLKIWHCVLTERFSNRCTLTTQSQSALPTLENSDHTESLENIMALTMRHAAASM 107
CHE14 SSD 351-472           ---VLLIAIGSDDAFLLKSNFP--------------------KHLNED-------T-FHTFLSHTSFTM 72
KIAA 1742 Mouse SSD 407-543 ---LLLSSVCANHTLIFFDLWR------LSK------------SQLPSG----GLAQRVGRTMHHFGYLL 87
PTC1 Mouse  SSD 424-584     VLPFLALGVGVDDVFLLAHAFS----ETGQNK----------RIPFEDR---------TGECLKRTGASV 111
PTC1 Human  SSD 438-598     VLPFLALGVGVDDVFLLAHAFS----ETGQNK----------RIPFEDR---------TGECLKRTGASV 111
PTC2 Mouse SSD 991-1113     ------IGIGVEFTVHVALGFL--------T------------SHGSRN-------LRAASALEQTFAPV 72
PTC2 Human SSD 394-552      VLPFLALGIGVDDVFLLAHAFT----EALPG------------TPLQER---------MGECLQRTGTSV 109
SCAP Human SSD 284-442      IFPYLVVVIGLENVLVLTKSVV------STP------------VDLEVK-------LRIAQGLSSESWSI 109
NPC1 Mouse SSD 621-786      VIPFLVLAVGVDNIFILVQTYQ------RDER----------LQEETLD-------QQLGRILGEVAPTM 116
NPC1 Human SSD 620-785      VIPFLVLAVGVDNIFILVQAYQ------RDER----------LQGETLD-------QQLGRVLGEVAPSM 116
HMGCR Human SSD 61-218      ALPFFLLLIDLSRASTLAKFAL------SSN------------SQDEVR-------ENIARGMAILGPTF 108

Consensus sequence          FLTSLSTAAAFFAGALSNIP-AVRCFSLFAGVAVLVNFALVLLWFPALLSL

Disp Mouse SSD 523-657     FVTSFTTAAAFYANYVSNIT-AIRCFGVYAGTAILVNYVLMVTWLPAVIVL                  135
Disp Human SSD 507-643      LVSGLTTSAAFYASYLSRLP-AVRCLALFMGTAVLVHLALTLVWLPASAVL                  137
Disp Dros SSD 468-624       FVTSLTTAGAFYASYSSSIT-AIKCFGIFAGTVVVTNYLLMITWLPASVSI                  157
CHE14 SSD 351-472           FLTCFSTIVPFFINITSNVI-VFRCFGLFAGVTVIFNYFMVVSFLPAFLLI                  122
KIAA 1742 Mouse SSD 407-543 LVSGLTTSAAFYASYLSRLP-AVRCLALFMGTAVLVHLALTLVWLPASAVL                  137
PTC1 Mouse  SSD 424-584     ALTSISNVTAFFMAALIPIP-ALRAFSLQAAVVVVFNFAMVLLIFPAILSM                  161
PTC1 Human  SSD 438-598     ALTSISNVTAFFMAALIPIP-ALRAFSLQAAVVVVFNFAMVLLIFPAILSM                  161
PTC2 Mouse SSD 991-1113     TDGAVSTLLGLLMLAGSNFDFIIRYFFVVLTVLTLLGLLHGLLLLPVLLSI                  123
PTC2 Human SSD 394-552      VLTSINNMAAFLMAALVPIP-ALRAFSLQAAIVVGCTFVAVMLVFPAILSL                  159
SCAP Human SSD 284-442      MKNMATELGIILIGYFTLVP-AIQEFCLFAVVGLVSDFFLQMLFFTTVLSI                  159
NPC1 Mouse SSD 621-786      FLSSFSETSAFFFGALSSMP-AVHTFSLFAGMAVLIDFLLQITCFVSLLGL                  166
NPC1 Human SSD 620-785      FLSSFSETVAFFLGALSVMP-AVHTFSLFAGLAVFIDFLLQITCFVSLLGL                  166
HMGCR Human SSD 61-218      TLDALVECLVIGVGTMSGVR-QLEIMCCFGCMSVLANYFVFMTFFPACVSL                  158
```

Fig. 1. Mouse dispatched (Disp) belongs to an emerging family of proteins containing a sterol-sensing domain (SSD). (A) Predicted 1521 amino acids translation product of the *Disp* gene. The SSD (blue) and the 12 putative transmembrane domains (red) are colored. Transmembrane domain prediction was performed using the TopPred2 program (http://www.sbc.su.se/~erikw/toppred2). (B) Amino acid alignment between SSD-containing proteins. In addition to dispatched, several other major classes of SSD-containing proteins are incorporated in the alignment, including patched 1 (PTC1 in figure), the Hh receptor (Goodrich et al., 1996); the sterol regulatory element-binding protein [SREBP]-cleavage activation protein (SCAP) (Brown and Goldstein, 1999; Goldstein and Brown, 1990); NPC1, a protein affected in the lipid storage disorder Niemann-Pick disease type C1 (Carstea et al., 1997; Loftus et al., 1997); and HMG CoA reductase (HMGCR), a cholesterol biosynthetic enzyme (Gil et al., 1985). Che-14 encodes a *C. elegans* orthologue of *disp* and is likely to be involved in apical secretions of proteins (Michaux et al., 2000). KIAA 1742 encodes the Disp-related protein and its function is unknown. Only the SSD domains are shown and conserved amino acid residues are shown in green. Numbers to the right of the genes represent the amino acid positions in the corresponding protein used in the sequence alignment. Sequence alignment was performed using the CLUSTAL W algorithm (Thompson et al., 1994) in the DNASTAR program.

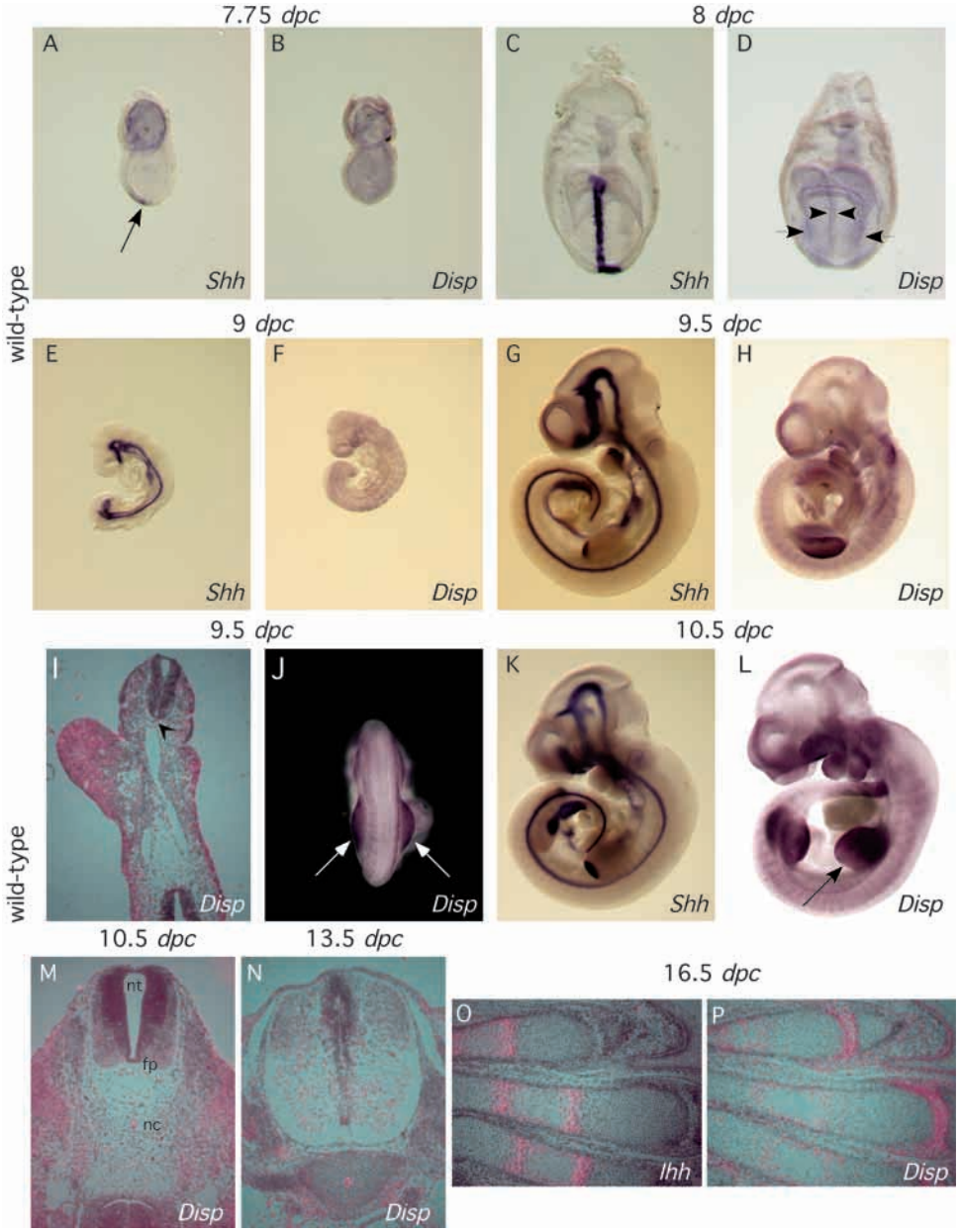

Fig. 2. Expression of *Disp* overlaps with *Hh* expression in the mouse embryo. (A-H,J-L) Whole-mount in situ hybridization, using digoxigenin-labeled *Shh* and *Disp* riboprobes on wild-type mouse embryos at different stages of development from 7.75 to 10.5 dpc. (I,M-P) Section in situ hybridization using ^{33}P-UTP-labelled *Disp* and *Ihh* riboprobes on paraffin wax sections of wild-type mouse embryos from 9.5 to 16.5 dpc. (A,B) Lateral view of late streak, head process stage egg cylinder (~7.75 dpc). Arrow in A indicates *Shh* expression in the node. (C,D) Ventral anterior view of head fold stage embryos just prior to somite formation (~8 dpc). Arrowheads in D indicate *Disp* expression in cells immediately adjacent to the midline mesoderm and arrows indicate *Disp* expression at junctions between neural and surface ectoderm. (E,F) Stage showing 13-20 somites (~9 dpc). Lateral view. (G,H) Stage showing 20-25 somites (~9.5 dpc). Lateral view. (I) Cross-section of a wild-type 9.5 dpc mouse embryo at the forelimb level. Arrowhead indicates the notochord. (J) Dorsal view of H at the forelimb level. White arrows indicates *Disp* expression in the forelimb buds. (K,L) Stage showing 31-35 somite (~10.5 dpc). Lateral view. (M) Cross-section of a wild-type 10.5 dpc mouse embryo at the forelimb level. (N) Cross-section of a wild-type 13.5 dpc mouse embryo through the thoracic cavity. (O,P) Longitudinal section through the metatarsal bones of the hindlimb of a wild-type 16.5 dpc mouse embryo. Phalanges (not shown) are to the right of the pictures. nt, neural tube; fp, floor plate; nc, notochord.

addition, *DispΔ E8* mutants fail to complete embryonic turning (Fig. 4B). The embryonic lethality observed in homozygous *DispΔ E8* mutants is most probably due to defective heart development. *DispΔ E8* mutants fail to undergo normal rightward looping of the heart, which remains as a linear tube and is surrounded by a bloated pericardial sac (Fig. 4B,F). All of these phenotypes have been reported in embryos defective in Hh signaling (Chiang et al., 1996; Zhang et al., 2001).

To confirm that the observed defects in *DispΔ E8* mutants are due to defective Hh signaling, we examined the expression of the Hh targets, *Ptch*, *Hip1* and *Gli1* (Chuang and McMahon, 1999; Goodrich et al., 1996; Marigo et al., 1996; Platt et al., 1997). In situ hybridization was used to monitor their expression in *DispΔ E8* mutants in wholemounts and sections. Expression of *Hip1* is known to be completely dependent on Hh signaling (Chuang and McMahon, 1999) while *Ptch* expression is initially Hh independent but is strongly upregulated upon Hh signal transduction (Goodrich et al., 1996). In *DispΔ E8* mutants at 9.5 dpc, *Shh* is expressed in the notochord, the ZPA, the gut endoderm and the branchial arches (Fig. 5B,J), but expression of *Hip1* (Fig. 5F) and *Gli1* (Fig. 5H) is completely absent in *DispΔ E8* mutants. Expression of *Ptch* is greatly reduced and only weak expression is detected in the sclerotome of the somite, the ventral neural tube and the distal posterior margin of the forelimb (Fig. 5D,L), which may reflect Hh-independent expression of *Ptch*. Taken together, these findings indicate that *Disp* is required for Hh signaling during mouse embryogenesis.

Disp mutants display multiple defects in LR axis determination and in the development of the axial structure, ventral neural tube, somite and limb, because of defective Hh signaling

To better understand the molecular mechanisms that underlie

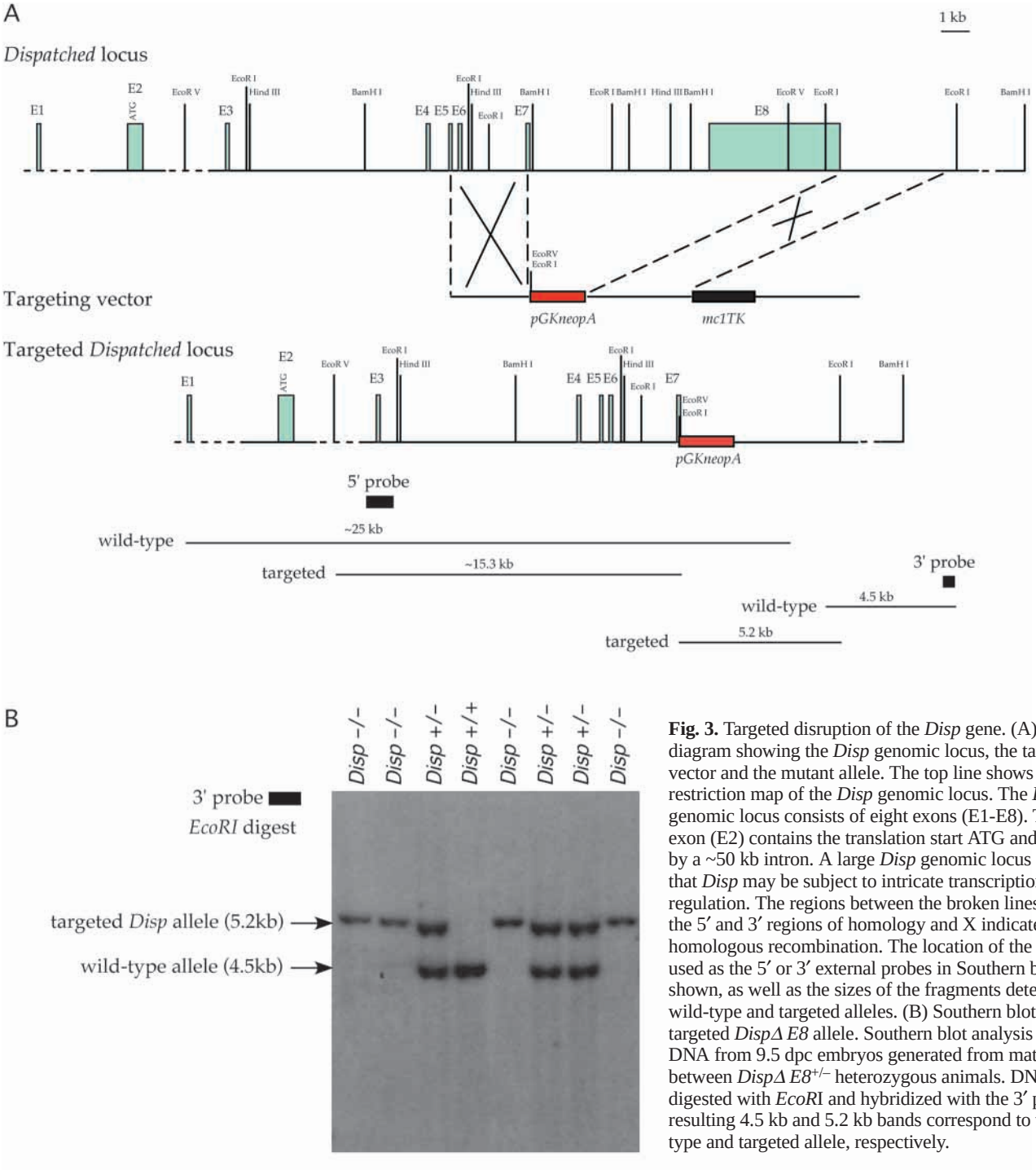

Fig. 3. Targeted disruption of the *Disp* gene. (A) Schematic diagram showing the *Disp* genomic locus, the targeting vector and the mutant allele. The top line shows a partial restriction map of the *Disp* genomic locus. The *Disp* genomic locus consists of eight exons (E1-E8). The second exon (E2) contains the translation start ATG and is followed by a ~50 kb intron. A large *Disp* genomic locus suggests that *Disp* may be subject to intricate transcriptional regulation. The regions between the broken lines represent the 5′ and 3′ regions of homology and X indicates events of homologous recombination. The location of the fragments used as the 5′ or 3′ external probes in Southern blotting are shown, as well as the sizes of the fragments detected for wild-type and targeted alleles. (B) Southern blot analysis of targeted *DispΔ E8* allele. Southern blot analysis of genomic DNA from 9.5 dpc embryos generated from matings between *DispΔ E8*$^{+/-}$ heterozygous animals. DNA was digested with *Eco*RI and hybridized with the 3′ probe. The resulting 4.5 kb and 5.2 kb bands correspond to the wild-type and targeted allele, respectively.

the defects observed in *DispΔ E8* mutant embryos, we performed a detailed histological and marker analysis. Our analysis focused on LR axis determination, the axial structures, the ventral neural tube, the somite and the limb, as the role Hh signaling plays in patterning these structures has been well characterized (Chiang et al., 1996; Lewis et al., 2001; Marti et al., 1995b; Riddle et al., 1993; Roelink et al., 1995; Zhang et al., 2001). In addition, formation of these structures involves both short- and long-range Hh signaling.

Disp mutants are first distinguishable at the six- to seven-somite stages (~8.5 dpc) by the abnormal morphology of the forebrain, indicative of loss of ventral midline fate, and by a delay in cardiac morphogenesis (data not shown). The failure to complete embryonic turning and the absence of heart looping in *DispΔ E8* mutants suggested that LR axis development may be affected, as has been previously reported in *Smo* mutants (Zhang et al., 2001). *Pitx2*, which encodes a bicoid-related homeobox protein, is expressed in the left lateral plate mesoderm (LPM) from two- to three-somite (~8 dpc) to 10 somite (8.5 dpc) stages in wild-type embryos (Piedra et al., 1998; Ryan et al., 1998; Yoshioka et al., 1998). *Pitx2* expression is greatly reduced in the left LPM in two- to six-

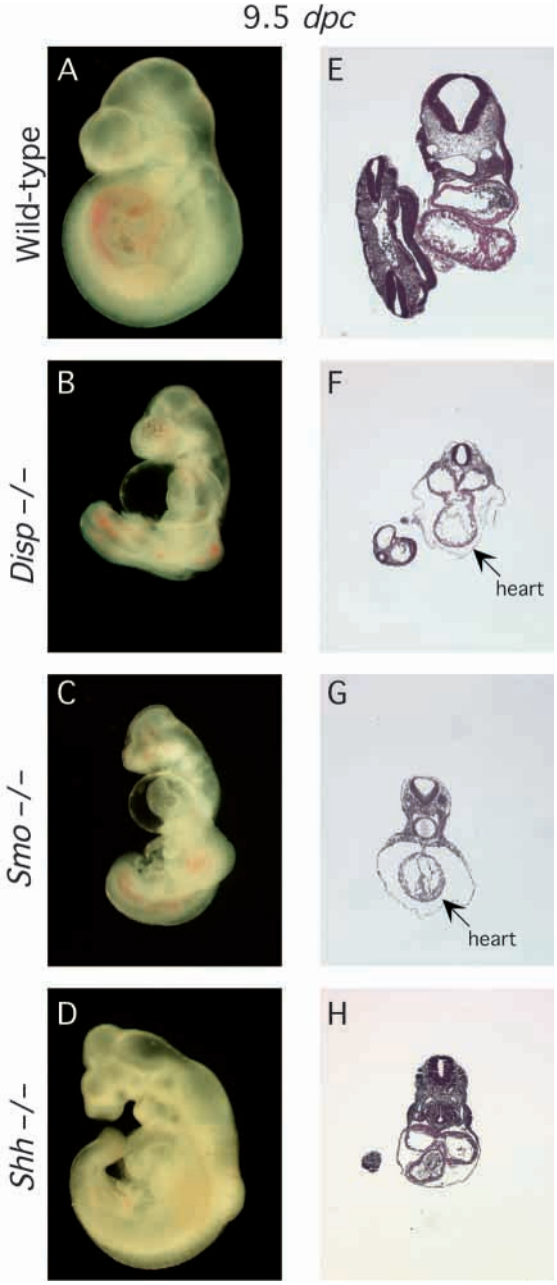

Fig. 4. *Disp* null mutants phenocopy *Smo* mutants. (A-D) External morphology of wild-type (A), *Disp*$^{-/-}$ (B), *Smo*$^{-/-}$ (C) and *Shh*$^{-/-}$ (D) embryos at 9.5 dpc. All views are lateral except B,C, which represent lateral ventral views. Note that embryos in B,C have initiated but failed to complete turning. By contrast, *Shh*$^{-/-}$ embryo (D) collected at a similar stage has completed embryonic turning. (E-H) Cross-sections of 9.5 dpc wild-type (E), *Disp*$^{-/-}$ (F), *Smo*$^{-/-}$ (G) and *Shh*$^{-/-}$ (H) embryos at the level of the heart tube stained with Hematoxylin and Eosin. Arrows in F,G indicate the linear heart tube in *Disp* (F) and *Smo* (G) mutants, when compared with the multichambered heart in the wild-type (E) and *Shh*$^{-/-}$ (H) embryos. All major cell types are present in a grossly normal organization in *Disp* mutants (F).

somite *DispΔ E8* mutants, whereas expression of *Pitx2* in the head mesenchyme and yolk sac is unaltered (data not shown). These results suggest that defective *Shh* and *Ihh* signaling in the node affects the establishment of LR asymmetry (Zhang et al., 2001) in *DispΔ E8* mutants.

Analysis of *Shh* mutant mice suggests that *Shh* is required for the maintenance but not the formation of the notochord (Chiang et al., 1996). If *Disp* is required for Hh signaling, phenotypes resembling the axial defects in *Shh* mutants should be observed in *DispΔ E8* mutants. Consistent with this hypothesis, expression of brachyury [which is required for differentiation of the notochord and is normally expressed in the primitive streak, the node and developing notochord (Herrmann and Kispert, 1994)] becomes discontinuous in the rostral region of *DispΔ E8* mutant embryos (arrow in Fig. 6B). Though the origin of the floor plate is not completely understood, the floor plate and notochord share similar expression profiles (including *Shh* and *Hnf3b*) and there is good evidence to suggest that expression of Shh in the notochord acts short-range to induce floor plate (Le Douarin and Halpern, 2000; Placzek et al., 2000). In *DispΔ E8* mutant embryos, *Shh* (Fig. 5B,J) and *Hnf3β* (Fig. 6D,F) are not detected in the ventral midline of the neural tube, suggesting that the floor plate fails to form. These results indicate that *Disp* is required for *Shh* signaling in the axial midline.

Shh signaling from both the notochord and the floor plate plays a key role in patterning the ventral neural tube in a dose-dependent manner (Chiang et al., 1996; Roelink et al., 1995). To examine whether dorsoventral patterning of the neural tube is affected in *DispΔ E8* mutants, we probed the expression of molecular markers that define different dorsoventral positions in the early neural tube (Briscoe and Ericson, 1999; Briscoe and Ericson, 2001). In the neural tube, *Pax3* expression is normally restricted to the dorsal half (alar plate) of the spinal cord from the tail to the diencephalons (Fig. 6G) and *Pax6* is only weakly expressed in the alar plate and more strongly throughout the ventral half (basal plate) of the neural tube, except at the ventral midline (Fig. 6I). In *DispΔ E8* mutants at 9.5 dpc, *Pax3* expression in the spinal cord extends ventrally (Fig. 6H), whereas *Pax6* expression level is quite low (to a level characteristic of normal alar plate expression) (Fig. 6J). *Wnt1* (data not shown) and *Wnt3a* (Fig. 6P) are expressed in the roof plate in *DispΔ E8* mutants. These results indicate that the ventral neural fate is not properly specified in the absence of *Disp*. Consistent with this conclusion, expression of a set of homeodomain proteins in neuroprogenitor cells (such as *Dbx1*, *Dbx2*, *Nkx6.1* and *Nkx2.2*) was not detected in *DispΔ E8* mutants (compare Fig. 6K with 6L and data not shown). Expression of these homeodomain genes is induced or repressed in response to graded *Shh* signaling (reviewed by Briscoe and Ericson, 1999; Briscoe and Ericson, 2001). Recent studies suggest that the resulting overlapping expression domains of these genes specify different neuronal types, including interneurons and motoneurons, at distinct positions of the ventral neural tube. Loss of the homeodomain code resulted in absence of islet 1 expression, a marker for motoneurons, in *DispΔ E8* mutants (Fig. 6N), as well as loss of *En1*, which is expressed in V1 interneurons (data not shown).

Many studies have shown that *Shh* signaling in the floor plate and notochord induces expression of sclerotomal marker *Pax1* and suppresses the dorsal dermomyotomal marker *Pax3* (Chiang et al., 1996; Fan et al., 1995; Fan and Tessier-Lavigne, 1994). In *DispΔ E8* mutants at 9.5 dpc, *Pax1* expression is

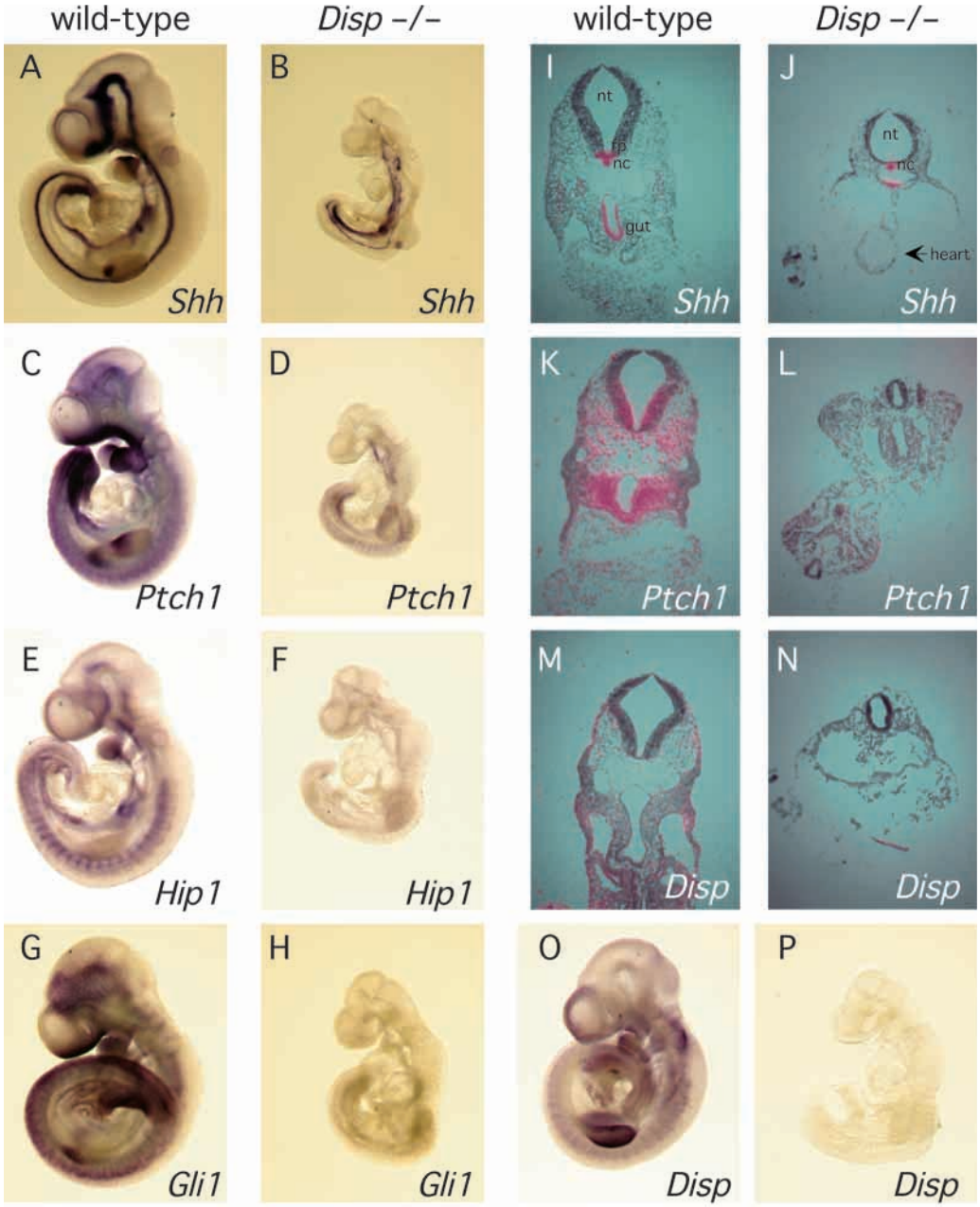

Fig. 5. *Disp* null mutants are defective in Hh signaling. (A-H,O-P) Whole-mount in situ hybridization using digoxigenin-labeled riboprobes on wild-type (A,C,E,G,O) and *Disp*$^{-/-}$ (B,D,F,H,P) embryos at 9.5 dpc. All views are lateral. (A,B) *Shh* expression; (C,D) *Ptch* expression; (E,F) *Hip1* expression; (G,H) *Gli1* expression; (O,P) *Disp* expression. (I-N) Isotopic section in situ using ^{33}P-UTP-labeled riboprobes on wild-type (I,K,M) and *Disp*$^{-/-}$ (J,L,N) embryos at 9.5 dpc. (J) Cross-section at the heart level. (I,K,L,M,N) Cross-sections at the forelimb level. (I,J) *Shh* expression; (K,L) *Ptch* expression; (M,N) *Disp* expression. nt, neural tube; fp, floor plate; nc, notochord.

not induced in the somite, suggesting that sclerotomal differentiation does not occur (Fig. 6R). By contrast, *Pax3* expression in the somite is expanded ventrally (Fig. 6H,T). We then asked whether dermomyotomal development is affected in the absence of *Disp*. In wild-type embryos, the first myogenic bHLH gene to be expressed is *Myf5* at 8 dpc (Summerbell et al., 2000), followed by the activation of myogenin at 8.5 dpc (Tajbakhsh et al., 1997). *Myod1* expression is detected about 2 days later at 9.75 dpc (Tajbakhsh et al., 1997). In *DispΔ E8* mutants at 9.5 dpc, *Myf5* was detected at low levels in the dermomyotome (Fig. 6V). Myogenin and *Myod1* expressions are not detected at these stages (Fig. 6X and data not shown). These results suggest that dermomyotomal development is initiated but does not proceed in *DispΔ E8* mutants.

Shh signaling from the ZPA specifies digit identity along the anteroposterior (AP) axis of the limb (Chiang et al., 1996; Lewis et al., 2001; Riddle et al., 1993; Yang et al., 1997). As described above, though *Shh* expression in the ZPA appears to be normal in the forelimb buds of *DispΔ E8* mutants at 9.5 dpc (Fig. 5B), Hh targets are either not induced (*Hip1* and *Gli1*) (Fig. 5F,H) or the expression levels are greatly reduced (*Ptch*) (Fig. 5D,L), suggesting that proper AP patterning is disrupted. Consistent with this, *Hand2* (*dHand*) expression, which normally shows broader, *Shh*-dependent expression over almost half of the AP axis at this stage (Charite et al., 2000) (indicated by the bracket in Fig. 6Y), is truncated in *DispΔ E8* mutants (arrow in Fig. 6Z). Interestingly, expression of *Hoxd13*, the most posteriorly restricted Hoxd family member that is regulated by *Shh* signaling (Zakany and Duboule, 1999) (Fig. 6AA), is only slightly reduced in *DispΔ E8* mutants (Fig. 6BB). *Shh* signaling is known to induce *Fgf4* expression in the

apical ectodermal ridge (AER), which regulates proximodistal (PD) outgrowth of the limb bud (reviewed by Martin, 1998) (Fig. 6CC). *Fgf4* also functions to maintain *Shh* expression in the ZPA. In *DispΔ E8* mutants at 9.5 dpc, *Fgf4* expression is not detected in the AER (Fig. 6DD). This could be due to retarded growth of the mutants as well as defective Hh signaling to induce *Fgf4* expression. By contrast, *Fgf8* expression in the AER of *DispΔ E8* mutants cannot be distinguished from that of wild-type embryos (reviewed by Martin, 1998) (Fig. 6EE,FF). Dorsoventral (DV) patterning of the limb appears to occur normally in *DispΔ E8* mutants (Parr and McMahon, 1995) (data not shown). Together, these findings indicate an absolute requirement of *Disp* in multiple aspects of Hh signaling.

Shh protein is properly processed but the distribution of Shh protein is restricted to its sites of synthesis in *Disp* mutants

Studies in *Drosophila* suggest that *disp* is involved in facilitating the movement of the cholesterol-modified form of Hh and does not affect Hh synthesis or processing (Burke et al., 1999). As *Shh* expression appears to be normal in *DispΔ E8* mutants, we asked whether processing of Shh to generate a cholesterol-modified N-terminal fragment of Shh also occurs normally in *DispΔ E8* mutants. On western blots, Shh antibodies recognized the unprocessed (upper arrow in Fig. 7) as well as the processed form of Shh (Shh-Np) (lower arrow in Fig. 7) in wild-type and *DispΔ E8*$^{+/-}$ embryos. Shh antibodies also recognized Shh-N, which migrates slower than Shh-Np on an SDS-PAGE. By contrast, neither the unprocessed form of Shh nor the processed Shh-Np or Shh-N could be detected in lysate from *Shh* mutant embryos. In lysates from *DispΔ E8*$^{-/-}$ embryos, a band running at the same position as Shh-Np was detected by Shh antibodies, suggesting that Shh processing occurs in the absence of *Disp*. In addition, the ratio of processed to unprocessed (a very small amount) (data not shown) form of Shh in *DispΔ E8*$^{-/-}$ embryos could not be distinguished from that of their wild-type littermates. These results suggest that Shh processing occurs normally in the absence of *Disp*.

To investigate whether the phenotype observed in *DispΔ E8* mutants is due to defective Hh movement, we examined the distribution of Shh protein in wild-type and *DispΔ E8*$^{-/-}$ embryos. Using the procedure described by Gritli-Linde et al., we found that in wild-type mouse embryos at 9.5 dpc, Shh immunoreactivity is strong in the notochord and extends outwards in a graded fashion (arrows in Fig. 8A), upwards towards the ventral neural tube along the extracellular matrix (arrowheads in Fig. 8A) as previously shown (Gritli-Linde et al., 2001) and downwards towards the branchial pouch (data not shown). Similar patterns of Shh immunoreactivity extending from the notochord were observed on embryo sections where the floor plate has not yet been induced (Gritli-Linde et al., 2001). In *DispΔ E8* mutant embryos at this stage, Shh immunoreactivity is confined to the notochord and no immunoreactivity is detected outside the notochord (Fig. 8B). By contrast, in *Smo* mutant embryos, Shh immunoreactivity is detected in the notochord and extends in a graded fashion though at a lower level than that in wild type (data not shown). Taken together, these results indicate that while *DispΔ E8* and *Smo* mutants share similar phenotypes, the underlying molecular defects are different. Hh transport appears to be normal in *Smo* mutants but Hh protein is not capable of transducing its signal in Hh-responding cells. By contrast, in the absence of *Disp*, processed Hh protein fails to be transported out of Hh-producing cells and Hh-responding cells never receive the Hh signal.

DISCUSSION

We cloned the mouse dispatched gene and showed that it encodes a putative multipasss membrane protein with an SSD domain. Our phenotypic analysis of *Disp* mutant mice demonstrated that *Disp* null mice phenocopy *Smo* null mice (Zhang et al., 2001), suggesting that *Disp* is essential for Hh signaling. This conclusion was further supported by a detailed molecular analysis of *Disp* knockout mice that exhibit defects characteristic of loss of Hh signaling. We also provide evidence to indicate that *Disp* is not required for Hh protein synthesis or processing but rather is involved in moving Hh protein out of its sites of synthesis. In summary, our results are consistent with studies of *Drosophila disp*, indicating a conserved mechanism of facilitating Hh protein movement that is essential for proper Hh signaling.

Mouse dispatched in Hh signaling

Disp exhibits a dynamic expression pattern during mouse embryogenesis. It is possible that regulation of *Disp* expression involves Hh signaling. Expression of *Disp* in midline axial structures is relatively weak, although analysis of *Disp* mutants strongly suggests that *Disp* plays an essential role in midline Hh signaling. In this case, it is not known whether *Disp* is required continuously for proper signaling of Hh protein as initial expression levels of *Disp* are low. In addition, *Disp* expression in the limb becomes downregulated in locations where *Shh* is upregulated. It is possible that *Disp* is not continuously required or a low level of *Disp* expression is sufficient for Hh transport. It is interesting to note that in many structures *Disp* is expressed at a lower level in regions of Hh expression and at a higher level adjacent to regions of Hh signaling. One possibility is that *Disp* could be involved in a feedback mechanism to modulate Hh signaling. Alternatively, expression of *Disp* outside Hh expression domains may imply a potential role in processes not mediated by Hh signaling.

Our mutant analysis revealed the essential role *Disp* plays in Hh signaling, including *Shh* and *Ihh* signaling. As the phenotypes observed in *Disp* mutants and *Smo* mutants are identical in our analysis, it is most likely that no Hh signal is transduced in the absence of *Disp*, despite the prominent expression of Hh protein. Hh signaling involves both short- and long-range signaling, and it is somewhat surprising that in *Disp* mutants even short-range signaling is defective. For example, induction of floor plate does not occur in *Disp* mutants, and this process requires direct cell-cell contact of ventral midline cells with the notochord and not long-range movement of Hh protein (Le Douarin and Halpern, 2000; Placzek et al., 2000). It is possible that the Hh protein is not presented to the cell surface in the absence of Disp, although the Hh protein is properly processed in the secretory pathway of Hh-producing cells. Alternatively, Disp may be required directly in short-range signaling once the Hh protein is localized on the cell

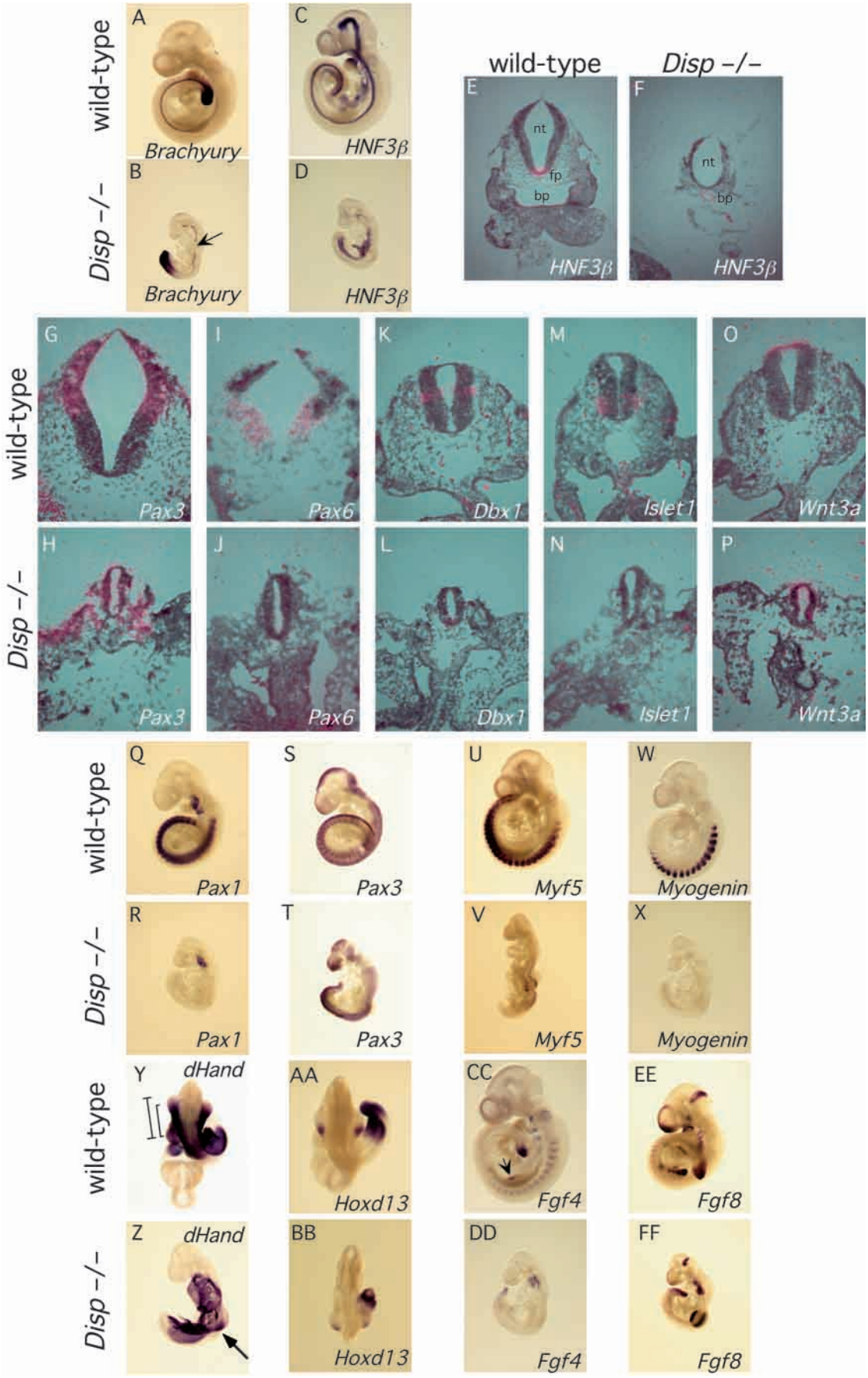
wild-type
Disp −/−
A
Brachyury
B
Brachyury
C
HNF3β
D
HNF3β
wild-type
Disp −/−
E
nt
fp
bp
HNF3β
F
nt
bp
HNF3β
wild-type
Disp −/−
G
Pax3
I
Pax6
K
Dbx1
M
Islet1
O
Wnt3a
H
Pax3
J
Pax6
L
Dbx1
N
Islet1
P
Wnt3a
wild-type
Disp −/−
Q
Pax1
S
Pax3
U
Myf5
W
Myogenin
R
Pax1
T
Pax3
V
Myf5
X
Myogenin
wild-type
Disp −/−
Y
dHand
AA
Hoxd13
CC
Fgf4
EE
Fgf8
Z
dHand
BB
Hoxd13
DD
Fgf4
FF
Fgf8

Fig. 6. *Disp* mutants exhibit multiple defects because of loss of Hh signaling. (A-D,Q-Z,AA-FF) Whole-mount in situ hybridization using digoxigenin-labeled riboprobes on wild-type (A,C,Q,S,U,W,Y,AA,CC,EE) and *Disp*$^{-/-}$ (B,D,R,T,V,X,Z,BB,DD,FF) embryos at 9.5 dpc. All views are lateral except (Y,Z,AA,BB), which represent dorsal views at the forelimb level. (A,B) Brachury (*T*) expression; (C,D) *Hnf3b* expression; (Q,R) *Pax1* expression; (S,T) *Pax3* expression; (U,V) *Myf5* expression; (W,X) myogenin expression; (Y,Z) *Hand2* (*dHand*) expression; (AA,BB) *Hoxd13* expression; (CC,DD) *Fgf4* expression; (EE,FF) *Fgf8* expression. Bracket in Y and arrow in Z indicate *Hand2* expression in the limb, whereas the line next to the bracket indicates the extent of the limb bud viewed at this angle. Arrow in CC indicates *Fgf4* expression in the posterior AER of the forelimb of a wild-type embryo. (E-P) Isotopic section in situ hybridization using ^{33}P-UTP-labeled riboprobes on paraffin sections of wild-type (E,G,I,K,M,O) and *Disp*$^{-/-}$ (F,H,J,L,N,P) embryos at 9.5 dpc. (E,F,I) Cross-section at the hindbrain level; (G,H,J-P) cross-section at the forelimb level. (E,F) *Hnf3b* expression; (G,H) *Pax3* expression; (I,J) *Pax6* expression; (K,L) *Dbx1* expression; (M,N) islet 1 expression; (O,P) *Wnt3a* expression. nt, neural tube; fp, floor plate; bp, branchial pouch.

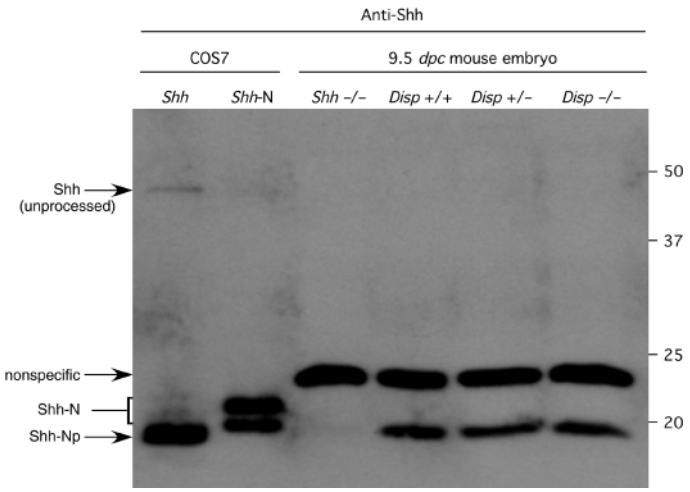

Fig. 7. Shh protein is processed in *Disp* mutant embryos. Western blot of lysate from wild-type, *DispΔ E8*$^{+/-}$, *DispΔ E8*$^{-/-}$, *Shh*$^{-/-}$ embryos collected at 9.5 dpc and COS7 cells transfected with expression constructs that encode either the full-length Shh protein (Shh) or the unmodified N-terminal fragment (Shh-N) probed with anti-Shh antibodies. Approximately equal amounts of proteins were loaded onto each lane. Both unprocessed (Shh,.upper arrow) and processed (Shh-Np, lower arrow) forms of Shh are detected from COS7 cells expressing the full-length Shh and are absent in lysate from *Shh* mutant embryos. A major band running at the same position as processed Shh was detected in lysate from wild-type, *DispΔ E8*$^{+/-}$ and *DispΔ E8*$^{-/-}$ embryos. The doublet observed in COS7 cells transfected with Shh-N could represent Shh-N proteins with different lipid modifications at its N terminus. A nonspecific band (or immunoreactivity with another Hh protein) was detected in lysates from embryos only and conveniently serves as a loading control. A very faint band representing the unprocessed Shh can be detected in lysates from wild-type, *DispΔ E8*$^{+/-}$ and *DispΔ E8*$^{-/-}$ embryos upon longer exposure (data not shown).

surface of Hh-producing cells. For example, Disp may be involved in partitioning Shh into membrane microdomains essential for Hh binding to Ptch or Disp may direct membrane to membrane transfer of Shh between Hh-producing and Hh-responding cells.

As *Disp* mutants do not survive beyond 9.5 dpc, it has not been possible to assess the role Disp plays in Ihh signaling in the developing chondrocytes and gut endoderm (Bitgood and McMahon, 1995; Ramalho-Santos et al., 2000; St-Jacques et al., 1999) as well as Dhh signaling in the developing testis and peripheral nerves (Bitgood et al., 1996; Parmantier et al., 1999). It is also possible that Disp has Hh-independent functions, because expression of Disp is detected in locations where none of the known Hh proteins is expressed. Answers to these issues will require further genetic and molecular studies.

A conserved mechanism of Hh transport in Hh-producing cells

Although the issue of lipid modification and its role in Hh movement in Hh-responding cells is not yet completely resolved, the crucial step of moving Hh protein out of Hh-producing cells appears to be evolutionarily conserved. Molecular analysis of *Drosophila disp* revealed its essential role in facilitating movement of the lipid-modified form of Hh protein in Hh-producing cells (Burke et al., 1999). Our studies demonstrate that the mouse ortholog of *Dispatched* also plays a similar role in Hh transduction. Because *Disp*-deficient mice phenocopy *Smo* mutants (Zhang et al., 2001), it is likely that *Disp* is involved in transporting all three mammalian hedgehog

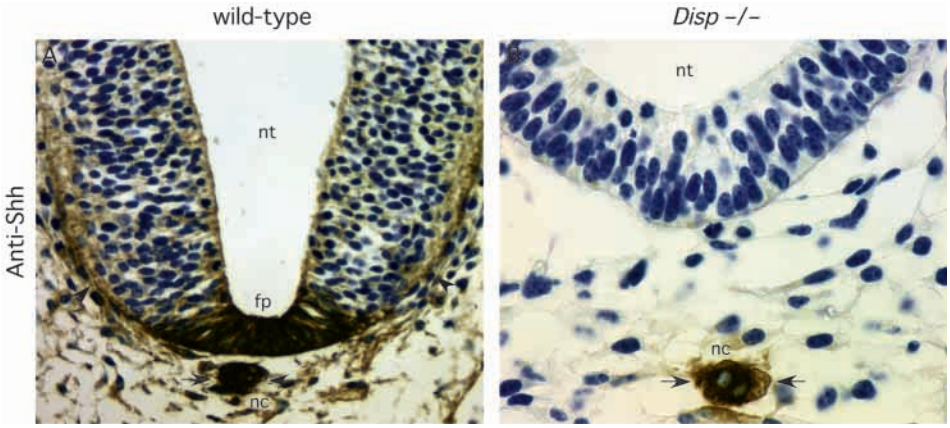

Fig. 8. Shh protein is restricted to its site of synthesis in *Disp* mutants. Cross-sections of wild-type (A) and *Disp*$^{-/-}$ (B) embryos at 9.5 dpc at the heart level. In the wild-type (A) sections, Shh immunoreactivity (brown) is strong in the notochord and floor plate and it extends out bi-directionally in a graded fashion (arrows and arrowheads). In sections of *Disp*$^{-/-}$ embryos (B), Shh immunoreactivity is only detected in the notochord (arrows) and no extended staining is present. nt, neural tube; fp, floor plate; nc, notochord.

proteins. These results suggest that the molecular mechanism by which lipid-modified Hh is released from Hh-producing cells is conserved. However, it is not known whether Disp is dedicated to facilitate the movement of lipid-modified Hh proteins or it also plays a role in transporting other lipid-modified proteins. The function of *Disp-related* is not known, but the fact that its restricted expression domain does not overlap with Hh expression (T'N. K. and P.-T. C., unpublished) suggests that *Disp-related* is unlikely to be involved in the same process as *Disp*.

Potential molecular mechanisms by which Disp mediates Hh movement

Generation of an active Hh signal is a highly regulated process. It involves autoproteolytic cleavage, lipid modification and regulated transport. Our studies show that Disp is not required for Hh protein synthesis or processing but rather is involved in moving Hh protein from its sites of synthesis. Mosaic analysis in *Drosophila* suggests that Disp is only required in Hh-producing cells but not in Hh-receiving cells to facilitate Hh movement, despite ubiquitous expression of *disp* mRNA (Burke et al., 1999). It is not known whether Disp also functions exclusively in Hh-producing cells for vertebrate Hh signaling. Compared with *disp*, mouse *Disp* exhibits a relatively restricted expression domain, although Disp protein distribution has not been determined. How Disp functions to facilitate Hh movement is also not known. Disp contains 12 predicted membrane-spanning domains but its subcellular localization remains to be determined. It is possible that Disp resides in the ER/Golgi to mediate the transport of Hh protein in the secretory pathway. Proteins with SSDs have been implicated in vesicular transport (Kuwabara and Labouesse, 2002) and Disp may be involved in a similar process to direct the movement of Hh-containing vesicles to the plasma membrane. Alternatively, Disp may function on the plasma membrane to promote the release of Hh protein from Hh-producing cells. Interestingly, the topology of Disp bears similarity to that of ion channels or transporters. Cellular and biochemical studies will be required to uncover the molecular mechanisms by which Disp facilitates transport of the lipid-modified form of Hh protein in Hh-producing cells.

We thank Dr Andy McMahon (Harvard University) for providing *Shh* and *Smo* mutant mice and all those who supplied probes. We thank Chris Wilson for help with sequence analysis, members of the Chuang laboratory for helpful discussion, and Chris Wilson, Tony Gerber, Didier Stainier, Shaun Coughlin and Tom Kornberg for critical reading of the manuscript. Work in the Chuang laboratory was supported by the Sandler Family Supporting Foundation, the HHMI Biomedical Research Support Program, March of Dimes Birth Defects Foundation and an NIH grant (HL67822).

REFERENCES

Bellaiche, Y., The, I. and Perrimon, N. (1998). Tout-velu is a Drosophila homologue of the putative tumour suppressor EXT-1 and is needed for Hh diffusion. *Nature* **394**, 85-88.

Bitgood, M. J. and McMahon, A. P. (1995). Hedgehog and Bmp genes are coexpressed at many diverse sites of cell-cell interaction in the mouse embryo. *Dev. Biol.* **172**, 126-138.

Bitgood, M. J., Shen, L. and McMahon, A. P. (1996). Sertoli cell signaling by Desert hedgehog regulates the male germline. *Curr. Biol.* **6**, 298-304.

Briscoe, J. and Ericson, J. (1999). The specification of neuronal identity by graded Sonic Hedgehog signalling. *Semin. Cell Dev. Biol.* **10**, 353-362.

Briscoe, J. and Ericson, J. (2001). Specification of neuronal fates in the ventral neural tube. *Curr. Opin. Neurobiol.* **11**, 43-49.

Brown, M. S. and Goldstein, J. L. (1999). A proteolytic pathway that controls the cholesterol content of membranes, cells, and blood. *Proc. Natl. Acad. Sci. USA* **96**, 11041-11048.

Bumcrot, D. A., Takada, R. and McMahon, A. P. (1995). Proteolytic processing yields two secreted forms of sonic hedgehog. *Mol. Cell. Biol.* **15**, 2294-2303.

Burke, R., Nellen, D., Bellotto, M., Hafen, E., Senti, K. A., Dickson, B. J. and Basler, K. (1999). Dispatched, a novel sterol-sensing domain protein dedicated to the release of cholesterol-modified hedgehog from signaling cells. *Cell* **99**, 803-815.

Carstea, E. D., Morris, J. A., Coleman, K. G., Loftus, S. K., Zhang, D., Cummings, C., Gu, J., Rosenfeld, M. A., Pavan, W. J., Krizman, D. B. et al. (1997). Niemann-Pick C1 disease gene: homology to mediators of cholesterol homeostasis. *Science* **277**, 228-231.

Charite, J., McFadden, D. G. and Olson, E. N. (2000). The bHLH transcription factor dHAND controls Sonic hedgehog expression and establishment of the zone of polarizing activity during limb development. *Development* **127**, 2461-2470.

Chiang, C., Litingtung, Y., Lee, E., Young, K. E., Corden, J. L., Westphal, H. and Beachy, P. A. (1996). Cyclopia and defective axial patterning in mice lacking Sonic hedgehog gene function. *Nature* **383**, 407-413.

Chuang, P.-T. and Kornberg, T. B. (2000). On the range of Hedgehog signaling. *Curr. Opin. Genet. Dev.* **10**, 515-522.

Chuang, P.-T. and McMahon, A. P. (1999). Vertebrate Hedgehog signalling modulated by induction of a Hedgehog-binding protein. *Nature* **397**, 617-621.

Echelard, Y., Epstein, D. J., St-Jacques, B., Shen, L., Mohler, J., McMahon, J. A. and McMahon, A. P. (1993). Sonic hedgehog, a member of a family of putative signaling molecules, is implicated in the regulation of CNS polarity. *Cell* **75**, 1417-1430.

Fan, C. M., Porter, J. A., Chiang, C., Chang, D. T., Beachy, P. A. and Tessier, L. M. (1995). Long-range sclerotome induction by sonic hedgehog: direct role of the amino-terminal cleavage product and modulation by the cyclic AMP signaling pathway. *Cell* **81**, 457-465.

Fan, C. M. and Tessier-Lavigne, M. (1994). Patterning of mammalian somites by surface ectoderm and notochord: evidence for sclerotome induction by a hedgehog homolog. *Cell* **79**, 1175-1186.

Gil, G., Faust, J. R., Chin, D. J., Goldstein, J. L. and Brown, M. S. (1985). Membrane-bound domain of HMG CoA reductase is required for sterol-enhanced degradation of the enzyme. *Cell* **41**, 249-258.

Goldstein, J. L. and Brown, M. S. (1990). Regulation of the mevalonate pathway. *Nature* **343**, 425-430.

Goodrich, L. V., Johnson, R. L., Milenkovic, L., McMahon, J. A. and Scott, M. P. (1996). Conservation of the hedgehog/patched signaling pathway from flies to mice: induction of a mouse patched gene by Hedgehog. *Genes Dev.* **10**, 301-312.

Gritli-Linde, A., Lewis, P., McMahon, A. P. and Linde, A. (2001). The whereabouts of a morphogen: direct evidence for short- and graded long-range activity of hedgehog signaling peptides. *Dev. Biol.* **236**, 364-386.

Harlow, E. and Lane, D. (1999). *Using Antibodies: A Laboratory Manual*. Cold Spring Harbor, NY: Cold Spring Harbor Laboratory Press.

Herrmann, B. G. and Kispert, A. (1994). The T genes in embryogenesis. *Trends Genet.* **10**, 280-286.

Ingham, P. W. and McMahon, A. P. (2001). Hedgehog signaling in animal development: paradigms and principles. *Genes Dev.* **15**, 3059-3087.

Joyner, A. L. (2000). *Gene Targeting: A Practical Approach*. Oxford: Oxford University Press.

Kalderon, D. (2000). Transducing the hedgehog signal. *Cell* **103**, 371-374.

Kuwabara, P. E. and Labouesse, M. (2002). The sterol-sensing domain: multiple families, a unique role? *Trends Genet.* **18**, 193-201.

Le Douarin, N. M. and Halpern, M. E. (2000). Discussion point. Origin and specification of the neural tube floor plate: insights from the chick and zebrafish. *Curr. Opin. Neurobiol.* **10**, 23-30.

Lee, J. J., Ekker, S. C., von Kessler, D. P., Porter, J. A., Sun, B. I. and Beachy, P. A. (1994). Autoproteolysis in hedgehog protein biogenesis. *Science* **266**, 1528-1537.

Lewis, P. M., Dunn, M. P., McMahon, J. A., Logan, M., Martin, J. F., St-Jacques, B. and McMahon, A. P. (2001). Cholesterol modification of sonic

hedgehog is required for long-range signaling activity and effective modulation of signaling by Ptc1. *Cell* **105**, 599-612.

Loftus, S. K., Morris, J. A., Carstea, E. D., Gu, J. Z., Cummings, C., Brown, A., Ellison, J., Ohno, K., Rosenfeld, M. A., Tagle, D. A. et al. (1997). Murine model of Niemann-Pick C disease: mutation in a cholesterol homeostasis gene. *Science* **277**, 232-235.

Marigo, V., Johnson, R. L., Vortkamp, A. and Tabin, C. J. (1996). Sonic hedgehog differentially regulates expression of GLI and GLI3 during limb development. *Dev. Biol.* **180**, 273-283.

Marti, E., Bumcrot, D. A., Takada, R. and McMahon, A. P. (1995a). Requirement of 19K form of Sonic hedgehog for induction of distinct ventral cell types in CNS explants. *Nature* **375**, 322-325.

Marti, E., Takada, R., Bumcrot, D. A., Sasaki, H. and McMahon, A. P. (1995b). Distribution of Sonic hedgehog peptides in the developing chick and mouse embryo. *Development* **121**, 2537-2547.

Martin, G. R. (1998). The roles of FGFs in the early development of vertebrate limbs. *Genes Dev.* **12**, 1571-1586.

Michaux, G., Gansmuller, A., Hindelang, C. and Labouesse, M. (2000). CHE-14, a protein with a sterol-sensing domain, is required for apical sorting in C. elegans ectodermal epithelial cells. *Curr. Biol.* **10**, 1098-1107.

Nichols, J., Evans, E. P. and Smith, A. G. (1990). Establishment of germ-line-competent embryonic stem (ES) cells using differentiation inhibiting activity. *Development* **110**, 1341-1348.

Parmantier, E., Lynn, B., Lawson, D., Turmaine, M., Namini, S. S., Chakrabarti, L., McMahon, A. P., Jessen, K. R. and Mirsky, R. (1999). Schwann cell-derived Desert hedgehog controls the development of peripheral nerve sheaths. *Neuron* **23**, 713-724.

Parr, B. A. and McMahon, A. P. (1995). Dorsalizing signal Wnt-7a required for normal polarity of D-V and A-P axes of mouse limb. *Nature* **374**, 350-353.

Pepinsky, R. B., Zeng, C., Wen, D., Rayhorn, P., Baker, D. P., Williams, K. P., Bixler, S. A., Ambrose, C. M., Garber, E. A., Miatkowski, K. et al. (1998). Identification of a palmitic acid-modified form of human Sonic hedgehog. *J. Biol. Chem.* **273**, 14037-14045.

Piedra, M. E., Icardo, J. M., Albajar, M., Rodriguez-Rey, J. C. and Ros, M. A. (1998). Pitx2 participates in the late phase of the pathway controlling left-right asymmetry. *Cell* **94**, 319-324.

Placzek, M., Dodd, J. and Jessell, T. M. (2000). Discussion point. The case for floor plate induction by the notochord. *Curr. Opin. Neurobiol.* **10**, 15-22.

Platt, K. A., Michaud, J. and Joyner, A. L. (1997). Expression of the mouse Gli and Ptc genes is adjacent to embryonic sources of hedgehog signals suggesting a conservation of pathways between flies and mice. *Mech. Dev.* **62**, 121-135.

Porter, J. A., Ekker, S. C., Park, W. J., von, K. D., Young, K. E., Chen, C. H., Ma, Y., Woods, A. S., Cotter, R. J., Koonin, E. V. et al. (1996a). Hedgehog patterning activity: role of a lipophilic modification mediated by the carboxy-terminal autoprocessing domain. *Cell* **86**, 21-34.

Porter, J. A., Young, K. E. and Beachy, P. A. (1996b). Cholesterol modification of hedgehog signaling proteins in animal development. *Science* **274**, 255-259.

Ramalho-Santos, M., Melton, D. A. and McMahon, A. P. (2000). Hedgehog signals regulate multiple aspects of gastrointestinal development. *Development* **127**, 2763-2772.

Riddle, R. D., Johnson, R. L., Laufer, E. and Tabin, C. (1993). Sonic hedgehog mediates the polarizing activity of the ZPA. *Cell* **75**, 1401-1416.

Roelink, H., Porter, J. A., Chiang, C., Tanabe, Y., Chang, D. T., Beachy, P. A. and Jessell, T. M. (1995). Floor plate and motor neuron induction by different concentrations of the amino-terminal cleavage product of sonic hedgehog autoproteolysis. *Cell* **81**, 445-455.

Ryan, A. K., Blumberg, B., Rodriguez-Esteban, C., Yonei-Tamura, S., Tamura, K., Tsukui, T., de la Pena, J., Sabbagh, W., Greenwald, J., Choe, S. et al. (1998). Pitx2 determines left-right asymmetry of internal organs in vertebrates. *Nature* **394**, 545-551.

Sambrook, J. and Russell, D. W. (2001). *Molecular Cloning: A Laboratory Manual*. Cold Spring Harbor, NY: Cold Spring Harbor Laboratory Press.

St-Jacques, B., Hammerschmidt, M. and McMahon, A. P. (1999). Indian hedgehog signaling regulates proliferation and differentiation of chondrocytes and is essential for bone formation. *Genes Dev.* **13**, 2072-2086.

Stickens, D., Clines, G., Burbee, D., Ramos, P., Thomas, S., Hogue, D., Hecht, J. T., Lovett, M. and Evans, G. A. (1996). The EXT2 multiple exostoses gene defines a family of putative tumour suppressor genes. *Nat. Genet.* **14**, 25-32.

Summerbell, D., Ashby, P. R., Coutelle, O., Cox, D., Yee, S. and Rigby, P. W. (2000). The expression of Myf5 in the developing mouse embryo is controlled by discrete and dispersed enhancers specific for particular populations of skeletal muscle precursors. *Development* **127**, 3745-3757.

Tajbakhsh, S., Rocancourt, D., Cossu, G. and Buckingham, M. (1997). Redefining the genetic hierarchies controlling skeletal myogenesis: Pax-3 and Myf-5 act upstream of MyoD. *Cell* **89**, 127-138.

Thompson, J. D., Higgins, D. G. and Gibson, T. J. (1994). CLUSTAL W: improving the sensitivity of progressive multiple sequence alignment through sequence weighting, position-specific gap penalties and weight matrix choice. *Nucleic Acids Res.* **22**, 4673-4680.

Wilkinson, D. G. and Nieto, M. A. (1993). Detection of messenger RNA by in situ hybridization to tissue sections and whole mounts. *Methods Enzymol.* **225**, 361-373.

Yang, Y., Drossopoulou, G., Chuang, P.-T., Duprez, D., Marti, E., Bumcrot, D., Vargesson, N., Clarke, J., Niswander, L., McMahon, A. et al. (1997). Relationship between dose, distance and time in Sonic Hedgehog-mediated regulation of anteroposterior polarity in the chick limb. *Development* **124**, 4393-4404.

Yoshioka, H., Meno, C., Koshiba, K., Sugihara, M., Itoh, H., Ishimaru, Y., Inoue, T., Ohuchi, H., Semina, E. V., Murray, J. C. et al. (1998). Pitx2, a bicoid-type homeobox gene, is involved in a lefty-signaling pathway in determination of left-right asymmetry. *Cell* **94**, 299-305.

Zakany, J. and Duboule, D. (1999). Hox genes in digit development and evolution. *Cell Tissue Res.* **296**, 19-25.

Zhang, X. M., Ramalho-Santos, M. and McMahon, A. P. (2001). Smoothened mutants reveal redundant roles for Shh and Ihh signaling including regulation of L/R symmetry by the mouse node. *Cell* **106**, 781-792.